Spatial Distribution Mapping by Mobile Sensor Networks: A Bayesian Method

Hyongju Park, Matthew Johnson-Roberson and Ram Vasudevan

Abstract—Constructing a spatially distributed map of environmental parameters such as hazardous chemical leakage, forest fires, or rain is a critical first step to effectively deploying intervention. Though such environmental mapping tasks could potentially be done efficiently via dispatching a group of autonomous agents, it is typically undertaken by humans due to the lack of formal methods that are able to guarantee satisfactory convergence to the true distribution. This paper presents a Bayesian approach to estimating spatially distributed target maps by deploying a group of mobile robots. The topological (locations) and spatial properties (e.g., radiation level, magnetic field strength, temperature levels, etc), which constitute the target state are unknown and are characterized by prior probability distribution over bounded domain. This paper proposes a deterministic motion model wherein robots move to maximize the observation likelihood based on their noisy sensor measurements and prior beliefs on target state. In addition, a decentralized counterpart, suitable for short range sensors, is presented wherein the workspace is partitioned into multiple disjoint regions, and each robot detects target only in its associated region. A suite of simulation results is presented to demonstrate the effectiveness of the proposed methods.

I. INTRODUCTION

A team of mobile robots equipped with ad-hoc communication and sensing devices, a *Mobile Sensor Network* (MSN), has a wide range of potential applications, including, exploration, surveillance, search and rescue missions, environmental monitoring for pollution detection and estimation, target tracking, cooperative detection of hazardous materials in contaminated environments, forest fire monitoring, oceanographic modeling, etc. [1]–[4]. Each such application can in fact be cast as a problem of trying to estimate some unknown, spatially distributed target of interest given some *a priori* measurement. Despite these numerous applications and the potential of MSNs to resolve environmental mapping, the lack of methods that are able to provide formal guarantees has meant that such environmental mapping has relied predominantly on human-controlled efforts. This paper aims to develop a class of sensing and motion model for MSNs to autonomously and collectively obtain an accurate representation of an arbitrary spatial target map under the Bayesian framework.

As a motivating example, consider the following scenario: a team of unmanned vehicles is deployed to monitor the radiation levels over a region of interest. Each vehicle is equipped with a close-range noisy radiation sensor, to inspect the radiation level over the region of interest. The vehicles must approach the radiation sources close enough to ensure accurate measurement while collectively building a radiation map over the entire region. To perform the required mission,

the group of vehicles must solve two problems: (i) *deployment*: the vehicles must be able to distribute themselves to maximize the likelihood that their collective measurements can be effectively combined to estimate the true target distribution; and (ii) *map reconstruction*: robots must be able to effectively update their posterior map using the prior believe on the map and new observations retrieved at the current configuration. *The objective of this paper is to design an effective, cooperative deployment and map reconstruction strategy for the robotic network.* This focuses on a group of homogeneous mobile robots equipped with range sensors tasked with building a spatial distribution map of a bounded domain where the data and the spatial coordinates of the data are correlated (e.g., precipitation map, heat distribution, radiation map, etc). This paper presents a novel sensor model along with a class of optimal multi-robot deployment strategies under Bayesian framework, and an approximate method via Particle Filtering for efficient environmental map reconstruction.

Bayesian inference has guided the development of a variety of tools to recursively estimate the state of a dynamical system and has as a result provided a powerful statistical tool to manage the measurement of uncertainties. In particular, during mobile robot search and exploration, the Bayesian method has enabled the construction of tools for the localization of targets [5], target tracking [6], POMDP planning [7], and source localization [8], [9] (e.g., aerosol, gas, sound, chemical plume, radiation sources). In this latter instance for example, the Bayesian approach led to the development of an autonomous search algorithm that maximized information gain to find a diffusive source [8]. We found that the key idea of their search algorithm to maximize over the information gain can be to adopted to solve our problem; the multi-agent environmental mapping. (Ram: Does your last sentence mean, that we are using their search algorithm but extending it the multi-agent case? If so, then please say that clearly.) (Hyongju: The multi-robot search problem of finding missing objects is a very different problem from ours. Our approach merely adopted their approach in that we are also maximizing over an information gain [positive detection likelihood] to determine our deployment policy. I edited the previous sentence to make this clear.)

Others have employed a non-Bayesian method to perform target distribution mapping using a single mobile robot [10]. This approach focused on trying to detect and identify gas concentration that was continuously distributed over a space. In this instance, the diffusive sensor, which is typically used in environmental mapping, was only able to provide information

about a relatively small area compared to their sonar or laser range scan counterparts. To overcome the limitation, the authors proposed a novel grid-mapped technique which used a Gaussian kernel to model the decreasing likelihood that a particular reading represents the true concentration with respect to the distance from the point of measurement. Despite the promising results, their method did not scale well in larger environment since it relied upon a single-robot that was deployed using a pre-specified Mowing pattern.

This paper is motivated by a similar environmental mapping objective; however our approach focuses on multi-robot probabilistic search for diffusive source using multi-robot deployment strategies [3]. While those studies of deployment assume a static, known prior topological target distribution, their goal is to find deployment policies that maximize the collective quantity of interest, e.g., Quality of Service (QoS), Signal-to-Noise Ratio (SNR). On the other hand, this presents a general framework for incremental reconstruction of spatially distributed target information map over a bounded region using new measurements made from a MSN, where sensors are dynamically reconfigured to maximize the most recent belief on the target distribution.

This paper's primary contributions are threefold: first, a probabilistic sensor model that incorporates joint target detection and spatial distribution estimation by a group of mobile sensors while capturing a key characteristic of the target detection task–the probability of seeing a target, monotonically decreases as a function of the distance between the sensor and the target, which is the common characteristics of range sensors (Ram: I still don't understand what you mean by: atypical property of range sensors. Are you trying to say that people don't typically assume that property for range sensors but it is a property of range sensors?). (Hyongju: My apologies again for not making this clear. I misunderstood the meaning of the word 'atypical'. I replaced the word with different one.) Second, a class of deployment strategies ranging from decentralized to fully coordinated ones where each control law is designed to maximize the observation likelihood marginalized over the previous belief of the target distribution. Finally, a variation of the Sequential Importance Resampling (SIR) Particle Filter which uses the joint observations and the updated configuration of the robots to update the posterior belief on the target by approximation.

Organizations: The rest of the paper is organized as follows. Section II presents notation used in the remainder of the paper, formally defines the problem of interest, and reviews a recursive Bayesian filter tailored to the problem. Section III presents a probabilistic sensor model. Section III studies the partitioned based approach to deployment, and the modified version of the sensor model discussed in Section IV. The deployment strategy is formally presented in Section V. Section VI discusses an approximate belief update method via particle filters. The effectiveness of this deployment and belief update approach is evaluated via numerical simulations in Sections VII. Finally, Section VIII concludes the paper and proposes a number of future directions.

II. METHOD FOR PROBABILISTIC MAPPING

This section presents the notation used throughout the paper, the problem of interest, and the recursive Bayesian filter.

A. Notations and Our System Definition

Throughout the text, the italic bold font is used to describe random quantities, a subscript t indicates that the value is measured at time step t, and $\mathbb{Z}^+$ denotes nonnegative integers. Given a continuous random variable $\boldsymbol{x}$, if it is distributed according to a Probability Density Function (PDF), we denote it by $f_{\boldsymbol{x}}$. Given a discrete random variable $\boldsymbol{y}$, if it is distributed according to a Probability Mass Function (PMF), we denote it by $p_{\boldsymbol{y}}$. Consider a group of m mobile robots deployed in a workspace, i.e., ambient space, $\mathcal{Q} \subseteq \mathbb{R}^d$. This paper assumes $d = 1, 2, 3$ though the presented framework generalizes. Let $\mathbb{S} = \{(x, y) \in \mathbb{R}^2 \mid x^2 + y^2 = 1\}$ be a *circle*, then the state of m robots is the set of locations and orientations at time t, and it is represented as an m-tuple $x_t = (x_t^1, \ldots, x_t^m)$, where $x_t^i \in \mathcal{Q} \times \mathbb{S}$. We denote by the set $x_{0:t} := \{x_0, \ldots, x_t\}$ the robot states up to time t. Given a pair of states (x_t, x_{t+1}), robots follow a way-point-based, continuous-time, deterministic motion model with dynamic constraints:

$$\dot{x}(t) = \mathrm{f}(x(t), u(t)) \tag{1}$$

with boundary conditions $x(t_0) = x_t$ and $x(t_f) = x_{t+1}$ where u is a control, t_0 is the *initial time*, and t_f is the *final time* which is free.

Let π_t be the *optimal control policy*[1] which drives robots' state from x_t to x_{t+1} in minimum time under the dynamic (or kinematic) constraints. We define a *target* to be a physical object or some measurable quantity spatially distributed over a bounded domain. Let $\boldsymbol{z}$ be the *target state* which is a random vector. The target state consists of location, $\boldsymbol{q} \in \mathcal{Q}$, and information states (quantitative information about the target), $\boldsymbol{I} \in \mathcal{I} \subseteq \mathbb{R}^n$. The Cartesian product $\mathcal{Z} = \mathcal{Q} \times \mathcal{I}$ is the *target state space*. Let the m-tuple $\boldsymbol{y}_t = (\boldsymbol{y}_t^1, \ldots, \boldsymbol{y}_t^m)$ be the observations recorded by m robots at time step t where $\boldsymbol{y}_t^i$ denotes the observation made by the ith sensor, and let the set $\boldsymbol{y}_{1:t} := \{\boldsymbol{y}_1, \ldots, \boldsymbol{y}_t\}$ denote observations made by m robots up to time t.

B. An Example: Precipitation Mapping

Before we formally define our problem, consider an real-world example. Suppose that one is interested in building the precipitation map of a city by collecting a group of autonomous vehicles' windshield wiper data (which provides high spatial and temporal resolution) as a preventive measure for flash floods. In this example, the information state is an instantaneous precipitation rate, and the target state is a location in the city. A proper choice of probabilistic observation model which captures the behavior of windshield wipers reasonably well, and a deployment strategy (where to send those vehicles)

---

[1]An example of such an optimal control could be the Linear-Quadratic Regulator if the dynamics were linear.

which maximizes the likelihood of rain detections, can be used as a sensor model, and motion model, respectively, to design a Recursive Bayesian Filter for estimating the true precipitation map. Such probabilistic method can be approximated, e.g., using Particle filter, for rapid reconstruction of the map.

C. Problem Definition

Let b_t represent a *belief*, the posterior probability distribution over the target state space at time $t \in \mathbb{Z}^+$. Each belief, b_t, depends on initial belief, b_0, the set of robot configurations, $\boldsymbol{x}_{0:t}$, and observations up to this point, $\boldsymbol{y}_{1:t-1}$. The state of robots are assumed completely *known*. Let $b^\star$ be the *true posterior belief*[2] on the target state. Then for each $t \in \mathbb{N}$, given the initial belief, b_0, our objective is obtain the sequence of optimal control policies $(\pi_1, \pi_2, \dots)$, each solves

$$\pi_t = \arg \max b_t, \qquad t = 1, 2, \dots, \qquad (2)$$

where each optimal policy between two time steps $[t, t+1)$, namely, π_t is subject to the dynamic constraints given in (1). To this end, we quantify the difference between the true posterior belief, $b^\star$ and an approximation using our method via the Kullback-Leibler (K-L) divergence. We demonstrate via our numerical simulation in Section VII that for a given $\epsilon > 0$, there is a dynamically varied stopping time $T > 0$ such that by the sequence of optimal policies, $(\pi_1, \dots, \pi_T)$, $t > T$ implies $D_{\mathrm{KL}}(b_t \| b^\star) < \epsilon$.

D. Recursive Bayesian Filter

We present an overview of the Bayesian filter, and the derivation of the filtering equations for our primary goal: spatial distribution mapping by m robots. We denote the belief about a given target state z at time $t \in \mathbb{N}$ as $b_t(z)$, and the belief of target information state $\boldsymbol{I}$ given the target located at q is given by:

$$b_t(I \mid \boldsymbol{q} = q) = f_{\boldsymbol{I} \mid b_0, x_{0:t}, \boldsymbol{y}_{1:t}, \boldsymbol{q}} (I \mid b_0, x_{0:t}, y_{1:t}, q) \quad (3)$$

where we denote the initial belief on target state by b_0. If the probability distribution about the target location, namely $f_{\boldsymbol{q}}$ is known *a priori*, the belief on the complete target state $\boldsymbol{z}$ is:

$$b_t(z) = f_{\boldsymbol{z} \mid b_0, \boldsymbol{y}_{1:t}} (z \mid b_0, x_{0:t}, y_{1:t})$$
$$= b_t(I \mid \boldsymbol{q} = q) f_{\boldsymbol{q}}(q). \quad (4)$$

If there is no prior knowledge of the target information at the initial time, one can choose the prior distribution as the *uniform* density. Applying *Bayes' theorem*, (3) becomes

$$b_t(I \mid \boldsymbol{q} = q)$$
$$= \frac{f_{\boldsymbol{y}_t \mid \boldsymbol{z}, b_0, x_{0:t}, \boldsymbol{y}_{1:t-1}} (y_t \mid z, b_0, x_{0:t}, y_{1:t-1}) \, b_{t-1}(I \mid \boldsymbol{q} = q)}{f_{\boldsymbol{y}_t \mid \boldsymbol{q}, b_0, x_{0:t}, \boldsymbol{y}_{1:t-1}} (y_t \mid q, b_0, x_{0:t}, y_{1:t-1})}$$

where $t \in \mathbb{N}$ Due to our sensor model (this is discussed in the next section), the observation $\boldsymbol{y}_t$ is conditionally independent of b_0, $\boldsymbol{y}_{1:t-1}$, and $x_{0:t-1}$ when it is conditioned on $\boldsymbol{z}$ and

---

[2] We assume for now that the true posterior target distribution can be obtained, e.g., via exhaustive search and measurements made by a MSN.

x_t One can simplify the likelihood function in the target information map by using this observation, which yields:

$$b_t(I \mid \boldsymbol{q} = q) = \eta_t \, f_{\boldsymbol{y}_t \mid \boldsymbol{z}, x_t} (y_t \mid z, x_t) \, b_{t-1}(I \mid \boldsymbol{q} = q) \quad (5)$$

where

$$\eta_t := \left(f_{\boldsymbol{y}_t \mid \boldsymbol{q}, b_0, x_{0:t}, \boldsymbol{y}_{1:t-1}} (y_t \mid q, b_0, x_{0:t}, y_{1:t-1}) \right)^{-1}$$

denotes the marginal probability, which is known as the *normalization constant*. This usually cannot be directly computed, but can be obtained by utilizing the total law of probability:

$$\eta_t = \left(\int_{\mathcal{I}} f_{\boldsymbol{y}_t \mid \boldsymbol{z}, x_t} (y_t \mid z, x_t) \, b_{t-1}(I \mid \boldsymbol{q} = q) \, dI \right)^{-1} \quad (6)$$

By joining the (4) and (5), one can obtain a simplified form of the filtering equation:

$$b_t(z) = \eta_t \, f_{\boldsymbol{y}_t \mid \boldsymbol{z}, x_t} (y_t \mid z, x_t) \, b_{t-1}(z) \quad (7)$$

$$= \left(\prod_{i=1}^{t} \eta_i f_{\boldsymbol{y}_i \mid \boldsymbol{z}, x_i} (y_i \mid z, x_i) \right) b_0(z). \quad (8)$$

We assume that m robots share their beliefs.

III. PROBABILISTIC RANGE SENSOR MODEL

Each mobile robot is equipped with a *range sensor* that can measure quantitative information from afar and a *radio* to communicate with other nodes to share its belief. Each range sensor measurement is corrupted by noise, and the measurement is valid only if the target is detected. This combined range sensor model joins the generic noisy sensor model with the binary sensor model [11]. In fact, this combined range sensor model has been experimentally validated during an object mapping and detection task using a laser scanner [12]. We postulate that this model is general enough to model other range sensors as well; as long as the sensor is capable of distinguishing the target from the environment, and has uniform sensing range. A few example sensors satisfying these characteristics are 360-degree camera, wireless antenna, Gaussmeter, heat sensor, olfactory receptor, etc.

During target detection, we assume each sensor returns a 0 if a target is detected or 1 otherwise. The ability to detect a target for each ith robot is a random variable $\boldsymbol{y}_B^i$ with a distribution that depends on the relative distance between the target and robot. This binary detection model, however, does not account for false positive or negatives. The probability of the event that all m sensors with configuration x_t fail to detect the target located at $q \in \mathcal{Q}$;

$$p_{\boldsymbol{y}_{B,t} \mid x_t, \boldsymbol{z}} (\boldsymbol{y}_{B,t} = \boldsymbol{0} \mid x_t, \boldsymbol{z} = (q, I)) \quad (9)$$

$$= p_{\boldsymbol{y}_{B,t} \mid x_t, \boldsymbol{q}} (\boldsymbol{y}_{B,t} = \boldsymbol{0} \mid x_t, \boldsymbol{q} = q) \quad (10)$$

$$= \prod_{i=1}^{m} p_{\boldsymbol{y}_{B,t}^i \mid x_t, \boldsymbol{q}} (\boldsymbol{y}_{B,t}^i = 0 \mid x_t, \boldsymbol{q} = q) \quad (11)$$

where $\boldsymbol{0} = (\underbrace{0, \dots, 0}_{m})$.

For measuring a quantity of interest from a given spatial distribution, we consider a generic, noisy sensor model,

where each sensor reports information regarding the environment, such as intensity data, as a *vector of reals*. Let $\boldsymbol{y}_I = (\boldsymbol{y}_I^1, \ldots, \boldsymbol{y}_I^n)$ be a n-random tuple for the measurements where n is the dimension of the sensor input. Without loss of generality, we assume that each random variable $\boldsymbol{y}_I^i$ has *range* $[I_{\min}^i, I_{\max}^i]$ where, $I_{\min}^i, I_{\max}^i \in \mathbb{R}$ for all $i \in \{1, \ldots, n\}$.

Let the random variable $\boldsymbol{y}_t = (\boldsymbol{y}_t^1, \ldots, \boldsymbol{y}_t^m)$ denote the *total observation* which is the collection of all observations reported by m sensors at time t, where each $\boldsymbol{y}_t^i$ is the Cartesian product of the two previously defined random vectors. Note that two random vectors $\boldsymbol{y}_B^i$ and $\boldsymbol{y}_I^i$ are *independent*[3] when conditioned on $x_t, \boldsymbol{z}$ so that joint PDF can be computed as:

$$f_{\boldsymbol{y}^i|\boldsymbol{z},x}(y^i \mid z, x) = p_{\boldsymbol{y}_B^i|\boldsymbol{z},x}(\boldsymbol{y}_B^i = y_B^i \mid z, x) f_{\boldsymbol{y}_I^i|\boldsymbol{z},x}(y_I^i \mid z, x) \tag{12}$$

where $y_B^i \in \{0, 1\}$. Since the set of observations $\boldsymbol{y}^1, \ldots, \boldsymbol{y}^m$ are made independently by m sensors, the joint probability distribution by m sensors, given a target at z becomes:

$$f_{\boldsymbol{y}_t|x_t,\boldsymbol{z}} (y_t \mid x_t, \boldsymbol{z} = z) = \prod_{i=1}^{m} f_{\boldsymbol{y}_t^i|x_t,\boldsymbol{z}} (y_t^i \mid x_t, \boldsymbol{z} = z) \tag{13}$$

$$= \prod_{i=1}^{m} p_{\boldsymbol{y}_{B,t}^i|x_t,\boldsymbol{z}} (\boldsymbol{y}_{B,t}^i = y_{B,t}^i \mid x_t, \boldsymbol{z} = z) \times$$
$$\prod_{i=1}^{m} f_{\boldsymbol{y}_{I,t}^i|x_t,\boldsymbol{z}} (y_{I,t}^i \mid x_t, \boldsymbol{z} = z) \tag{14}$$

$$= p_{\boldsymbol{y}_{B,t}|x_t,\boldsymbol{z}} (\boldsymbol{y}_{B,t} = y_{B,t} \mid x_t, \boldsymbol{z} = z) \times$$
$$f_{\boldsymbol{y}_{I,t}|x_t,\boldsymbol{z}} (y_{I,t} \mid x_t, \boldsymbol{z} = z) . \tag{15}$$

IV. PARTITION-BASED DEPLOYMENT APPROACH

Due to the limitation of the effective sensing range found on physical range sensors, we consider a partitioned-based strategy where the workspace is partitioned into m disjoint regions, and each robot is assigned to a region where it confines its detections This so called partitioned-based strategy is common to multi-robot coverage problems [3], [13]–[15]. The most popular one is based on the Voronoi tessellations (see e.g., [3], which we call a *non-coordinated strategy*). There are, in fact more general methods, which partition the workspace into p regions and assign $k \in [2, m]$ robots each region (note that if $k = m$, the method becomes *centralized*) [13]. By doing so, one can ensure that each target has a chance to be detected by at least one of the k sensors. This approach, which we call the *coordinated strategy*, can provide relative robustness by varying the value of k from 1 to m. Thus, if each sensor has an effective sensing range long enough to cover the whole workspace, utilizing all m sensors to detect every target in the workspace becomes the most desirable strategy.

A. The Optimal Partition

Consider m sensors and a workspace partition of $\mathcal{Q}$ into l disjoint regions, W such that $W = (W_1, \ldots, W_l)$, where

$\cup_i W_i = \mathcal{Q}$, and $W_i \cap W_j = \emptyset$ for all i, j pairs with $i \neq j$. Suppose the target location is a random variable $\boldsymbol{z}$ with PDF $\phi : \mathcal{Q} \to \mathbb{R}_{\geq 0}$. For a given target $z \in \mathcal{Q}$, we define the probability that a sensor located at x fails to detect target, using a real-valued function $h(\|z - x_i\|)$ as a probability measure[4], which is assumed to decrease monotonically as a function of the distance between the target and the ith sensor. Consider a bijection ^kG that maps a region to a set of k-points where the pre-superscript k explicitly states that the region is mapped to exactly k points. Additionally we make the following definitions:

Definition 4.1 (An Order$-k$ Voronoi Partition [16])**.** *Let x be a set of m distinct points in $\mathcal{Q} \subseteq \mathbb{R}^d$. The* order-$k$ Voronoi partition *of $\mathcal{Q}$ based on x, namely ^kV, is the collection of regions that partitions $\mathcal{Q}$ where each region is associated with the k nearest points in x.*

We also define another bijection $^kG^\star$ that maps a region to a set of k *nearest* points (out of x) to the region. The total probability that all m sensors fail to detect a target drawn by a distribution ϕ from $\mathcal{Q}$ is:

$$\int_{\mathcal{Q}} p_{\boldsymbol{y}_B|x,\boldsymbol{q}} (\boldsymbol{y} = \boldsymbol{0} \mid x, \boldsymbol{q} = q) \phi(q) \, dq. \tag{16}$$

By substituting $\mathcal{Q}$ with the workspace partition W, and $p_{\boldsymbol{y}_B|x,\boldsymbol{q}} (\boldsymbol{y} = \boldsymbol{0} \mid x, \boldsymbol{q} = q)$ with likelihood function h, we have

$$H(x, W, {}^kG)$$
$$= \sum_{j=1}^{l} \int_{W_j} \left(\prod_{x_i \in {}^kG(W_j)} (1 - h(\|q - x_i\|)) \right) \phi(q) \, dq \tag{17}$$

where we note again that the joint missed-detection events are conditionally independent, if conditioned on x. In fact, the order-k Voronoi tessellation is the optimal workspace partition which minimizes H for each choice of x and k:

Theorem 4.1 ([15])**.** *For a given x and k, $H(x, {}^kV, {}^kG^\star) \leq H(x, W, {}^kG)$ for all W, ^kG.*

Note that the order-k Voronoi partition V_k, along with the map $G_k^\star$ are uniquely determined given x, ϕ, and $\mathcal{Q}$.

B. Partitioned Range-limited Sensor Model

This section presents a practical sensor model that is better suited to distributed target detection based on the order-k Voronoi partition. The modified sensor model is a combination of deterministic workspace partitioning method and the probabilistic sensor model presented in Section III. In addition, we introduce another constraint for the model, namely the *effective sensing range*, $r_{\text{eff}} > 0$, to take into account the fact that the noisy measurement taken by each sensor does not depend on its distance to the target, if the target is sufficiently close to

---

[3]This assessment is based on the underlying assumption that the detection event and sensor measurement event are independent to each other.

[4]For the numerical simulations purpose, we further assume that $h(\cdot)$ is continuously differentiable function non-increasing on its domain, and the image of h must be in $[0, 1]$ for it to be a probability measure.

the sensor[5]. For a given k, and $z = (q, I)$, we assume that the following is true for our new sensor model:

Positive detection likelihood:

$p_{\boldsymbol{y}_{B,t}^i|\boldsymbol{z},x_t} \left(\boldsymbol{y}_t^i = 1 \mid x_t, z\right)$

$= \begin{cases} h\left(\|q - x_t^i\|\right) \times & \text{if } q \in {}^k G_t^\star(x_t^i) \cap \mathcal{B}(x_t^i, r_{\text{eff}}), \\ f_{\boldsymbol{y}_{I,t}^i|x_t,\boldsymbol{z}}(y_{I,t}^i \mid x_t, z), \\ 0, & \text{otherwise}, \end{cases}$

Negative detection likelihood:

$p_{\boldsymbol{y}_{B,t}^i|\boldsymbol{z},x_t} \left(\boldsymbol{y}_t^i = 0 \mid x_t, z\right)$

$= \begin{cases} \left(1 - h\left(\|q - x_t^i\|\right)\right) \times & \text{if } q \in {}^k G_t^\star(x_t^i) \cap \mathcal{B}(x_t^i, r_{\text{eff}}), \\ f_{\boldsymbol{y}_{I,t}^i|x_t,\boldsymbol{z}}(y_{I,t}^i \mid x_t, z), \\ 1, & \text{otherwise}, \end{cases}$

$\hspace{10cm} (18)$

where $\mathcal{B}(x, r)$ is an open ball with radius r centered at x.

V. Deployment strategy

As discussed in Section III, a measurement for a target is valid only if the target is detected. Thus, we consider a deployment strategy where robots move to locations maximizing their marginal likelihood of *positive* detections over the previous belief on the target state. Note that the marginal likelihood of positive detection is obtained by taking integrals on the positive likelihood estimate over the prior target distribution.

For $t \geq 2$ and sensors located at x_t, let l_t^+ be the positive likelihood that targets are detected by at least one sensor, then:

$l_t^+(x_t) := \int_{\mathcal{Z}} p_{\boldsymbol{y}_{B,t-1}|x_t,\boldsymbol{z}}\left(\boldsymbol{y}_{B,t-1} \neq \boldsymbol{0} \mid x_t, z\right) \times$
$\hspace{1cm} f_{\boldsymbol{y}_{I,t-1}|x_t,\boldsymbol{z}}\left(y_{I,t-1} \mid x_t, z\right) b_{t-2}(z) dz. \quad (19)$

Similarly, let l_t^- be the negative likelihood that target are missed detected by m sensors which is:

$l_t^-(x_t) := \int_{\mathcal{Z}} p_{\boldsymbol{y}_{B,t-1}|x_t,\boldsymbol{z}}\left(\boldsymbol{y}_{B,t-1} = \boldsymbol{0} \mid x_t, z\right) \times$
$\hspace{1cm} f_{\boldsymbol{y}_{I,t-1}|x_t,\boldsymbol{z}}\left(y_{I,t-1} \mid x_t, z\right) b_{t-2}(z) dz. \quad (20)$

We are interested in maximizing the likelihood of positive observation. Unfortunately, the integral term has a combinatorial number of terms, so it is impractical to compute (19) for large m. Instead we employ an alternative approach. First note the following:

Lemma 5.1. $\arg\min l_t^+(x_t) = \arg\min l_t^-(x_t)$

The proof of this lemma follows from the law of total probability and is omitted. According to Lemma 5.1, maximizing the likelihood that at least one sensor detects every target in the workspace, given the previous target belief, is identical to

---

[5]Recall that in our proposed sensor model, we assumed two tasks, detection and measurement, to be completely decoupled, nevertheless our generic noisy sensor model—which which treats all measurements taken within its maximum sensor range equally—can also be generalized to other popular forms (e.g., Gaussian, radially non-uniform, anisotropic, etc.)

minimizing the likelihood that all m sensors fail to detect a target in $\mathcal{Q}$.

Let $x_t^\star := \arg\min l_t^+(x_t) = \arg\min l_t^-(x_t)$, then:

$x_t^\star = \arg\min \left\{ \int_{\mathcal{Z}} p_{\boldsymbol{y}_{B,t-1}|x_t,\boldsymbol{q}}(\boldsymbol{y}_{B,t-1} = \boldsymbol{0} \mid x_t, z) \times \right.$
$\hspace{2cm} \left. p_{\boldsymbol{y}_{I,t-1}}(y_{I,t-1} \mid z) b_{t-2}(z) \right\} dz \quad (21)$
$= \arg\min \left\{ \int_{\mathcal{Q}} p_{\boldsymbol{y}_{B,t-1}|x_t,\boldsymbol{q}}(\boldsymbol{y}_{B,t-1} = \boldsymbol{0} \mid x_t, q) \times \right.$
$\hspace{2cm} \left. \int_{\mathcal{I}} p_{\boldsymbol{y}_{I,t-1}|\boldsymbol{z}}(y_{I,t-1} \mid z) b_{t-2}(z) \, dI \, dq \right\} \quad (22)$

where the detection likelihood is conditionally independent on $\boldsymbol{I}$ if conditioned on x and $\boldsymbol{q}$. We note that the maximum of the positive observation likelihood depends not only on the distance between targets and the robots, but also on the likelihood of the noisy sensor measurements. Thus, given the prior belief and the observations, robots find and move to new locations, and the posterior belief is updated at the new locations given the collected information. We define a new belief that joins the previous belief with the current measurement likelihood as:

$\widetilde{b}_{t-1}(q) := \int_{\mathcal{I}} p_{\boldsymbol{y}_{I,t-1}|\boldsymbol{z}}(y_{I,t-1} \mid z) b_{t-2}(z) \, dI$

$= \underbrace{f_{\boldsymbol{q}}(q)}_{\text{PDF of } \boldsymbol{q}} \underbrace{\int_{\mathcal{I}} p_{\boldsymbol{y}_{I,t}|\boldsymbol{z}}(y_{I,t} \mid \boldsymbol{z} = (q, I)) b_{t-2}(I \mid q) \, dI}_{\text{marginal likelihood of } \boldsymbol{y}_{I,t} \text{ conditioned on } q},$
$\hspace{10cm} (23)$

and a cost function

$L(x_t, y_{t-1}, \widetilde{b}_{t-1}) :=$
$\int_{\mathcal{Q}} p_{\boldsymbol{y}_{B,t-1}|x_t,\boldsymbol{q}}\left(\boldsymbol{y}_{B,t-1} = \boldsymbol{0} \mid x_t, q\right) \widetilde{b}_{t-1}(q) dq \quad (24)$

which illustrates the explicit dependence on the previous belief $\widetilde{b}_{t-1}$ and previous observations y_{t-1}. Then, our problem becomes

$x_t^\star = \arg\min_{x_t} L(x_t, y_{t-1}, \widetilde{b}_{t-1}). \quad (25)$

We note that for a given k, by substituting $\widetilde{b}_{t-1}$, x_t, y_{t-1} with ϕ, x, y respectively, and plugging observation likelihood functions from (18) and (24) becomes identical to $H(x, W, G^k)$ which was previously defined in (17). If the perception model is differentiable, our deployment strategy can use the gradient: $\nabla_{x_t} L(x_t, y_{t-1}, \widetilde{b}_{t-1})$ to find the desirable locations of the robots to maximize the observation likelihood as described in Algorithm 1. We use $\hat{x}_t$ to denote the suboptimal solution obtained by the gradient algorithm at time t.

Theorem 5.1. *Algorithm 1 is convergent.*

The formal proof of Theorem 5.1 is similar to the proof contained in our previous paper [15], and is thus omitted.

VI. Belief Approximation by Particle Filtering

We consider the Particle Filtering approach to reduce the complexity of the map reconstruction process.

Algorithm 1: Gradient Algorithm (MMLE)

Input: L, x_{t-1}, $\epsilon > 0$, $\widetilde{b}_{t-1}$, y_{t-1}
Output: $\hat{x}_t$
$k \leftarrow 0$, $x_{t,k} \leftarrow x_{t-1}$, $\delta L \leftarrow \epsilon$
while $\delta L > \epsilon$ **do**
    foreach $i \in \{1, \dots, m\}$ **do**
        $x^i_{t,k+1} \leftarrow x^i_{t,k} - \alpha^i_{t,k} \nabla_{x^i_t} L(x_t, y_{t-1}, \widetilde{b}_{t-1})$
        // $\alpha^i_{t,k}$ is obtained using a line search method
    $\delta L \leftarrow L(x_{t,k}, y_{t-1}, \widetilde{b}_{t-1}) - L(x_{t,k+1}, y_{t-1}, \widetilde{b}_{t-1})$
    $k \leftarrow k + 1$
return $\hat{x}_t \leftarrow x_{t,k}$

A. Low Discrepancy Sampling

For our numerical simulations, we consider a low discrepancy sampling method (e.g., Halton-Hammersley sequence [17]) to sample continuously distributed targets in $z \in \mathcal{Z} = \mathcal{Q} \times I$. This approach has been used for sampling-based algorithms for robot motion planning [18].

B. SIR Particle Filter

We consider Sequential Importance Resampling (SIR) [19] for the particle filtering process. For a given distribution on target locations, $f_{\boldsymbol{q}}(q)$, at each time t, based on the observations, the locations belief hypothesis is populated for N_1 samples initially generated with Halton-Hammersley sequence.

$$\left\{ \left(q^1_t, \widetilde{w}^1_{T,t} \right), \dots, \left(q^{N_1}_t, \widetilde{w}^{N_1}_{T,t} \right) \right\} \qquad (26)$$

where for each $i \in \{1, \dots, N_1\}$,

$$\widetilde{w}^i_t = p_{\boldsymbol{y}_{B,t}|\hat{x}_t, \boldsymbol{z}} \left(y_{B,t} \mid \hat{x}_t, \boldsymbol{z} = (q^i_t, I) \right) \qquad (27)$$

for all $I \in \mathcal{I}$. In a similar manner, for each sample q^i_t the information belief hypothesis is populated for N_2 samples from $\mathcal{I}$ initially generated by by the Halton-Hammersley sequence:

$$\left\{ \left(I^{i1}_t, \widetilde{w}^{i1}_{I,t} \right), \dots, \left(I^{iN_2}_t, \widetilde{w}^{iN_2}_{I,t} \right) \right\} \qquad (28)$$

where for each $i = 1, \dots, N_1$, $\sum_{j=1}^{N_2} w^{ij}_{I,t} = 1$, and

$$\widetilde{w}^{ij}_{I,t} \propto p_{\boldsymbol{y}_{I,t}|\hat{x}_t, \boldsymbol{z}} \left(y_{I,t} \mid \hat{x}_t, \boldsymbol{z} = (q^i, I^{ij}) \right) \qquad (29)$$

for all $i \in \{1, \dots, N_1\}$. If we let $z^{ij} := (q^i, I^{ij})$ and $\widetilde{w}^{ij}_t := \widetilde{w}^i_{T,t} \widetilde{w}^{ij}_{I,t}$ then the final expression for the set of $N := N_1 N_2$ particle-weight pairs at time t is

$$\left\{ \left\{ (z^{ij}, \widetilde{w}^{ij}_t) \right\}_{j=1}^{N_2} \right\}_{i=1}^{N_1} = \left\{ z^k, \widetilde{w}^k_t \right\}_{k=1}^{N} \qquad (30)$$

After resampling and normalizing, the approximate posterior belief becomes

$$\hat{b}_t(z) = \sum_{k=1}^{N} w^k_t \delta(z_t - z^k_t) \qquad (31)$$

which is a form of discrete random measure where the $w^1_t, \dots, w^N_t$ are resampled, normalized weight such that $\sum_{k=1}^{N} w^k = 1$, and $\delta(z_t - z^k_t)$ is Dirac-delta function evaluate

at z^k_t. We note that resampling is only taken on the target information state, namely, $\boldsymbol{I}_t$. The whole filtering process is depicted in Algorithm 2. Note that as discussed in previous studies [20], our particle filter uses standard re-sampling scheme to ensure the convergence of the mean square error toward zero with a convergence rate of $1/N_2$ for all $q \in \mathcal{Q}$.

Algorithm 2: Filtering Algorithm

Input: $\hat{b}_{t-1} = \{z^l, w^l_{t-1}\}_{l=1}^{N} =$
    $\{\{(q^i, I^{ij}), w^i_{B,t-1} w^{ij}_{I,t-1}\}_{j=1}^{N_2}\}_{i=1}^{N_1}, y_{t-1}, y_t, \hat{x}_{t-1}$
Output: $\hat{b}_t$
// Propogate motion model using MMLE (maximum marginal likelihood estimation); see Algorithm 1
$\hat{x}_t \leftarrow \text{MMLE}(\hat{b}_{t-1}, y_{t-1}, \hat{x}_{t-1})$
// SIR Particle Filter
// 1) Update using the observation model
foreach $i \in \{1, \dots, N_1\}$ **do**
    $\widetilde{w}^i_{B,t} \leftarrow p_{\boldsymbol{y}_{B,t}|\hat{x}_t, \boldsymbol{q}} \left(y_{B,t} \mid \hat{x}_t, \boldsymbol{q} = q^i_t \right)$
    foreach $j \in \{1, \dots, N_2\}$ **do**
        $\widetilde{w}^{ij}_{I,t} \leftarrow p_{\boldsymbol{y}_{I,t}|\hat{x}_t, \boldsymbol{z}} \left(y_{I,t} \mid \hat{x}_t, \boldsymbol{z} = (q^i, I^{ij}) \right)$

// 2) Resample and Normalize
$\{w^l_t\}_{l=1}^{N} \leftarrow \text{Resample}(\{\widetilde{w}^l_t\}_{l=1}^{N}, \{w^l_{t-1}\}_{l=1}^{N})$
return $\hat{b}_t \leftarrow \{z^l, w^l_t\}_{l=1}^{N}$
// Low Variance Resampling [21]
function Resample($\{\widetilde{w}^l_t\}_{l=1}^{N}, \{w^l_{t-1}\}_{l=1}^{N}$)
    forall $i \in \{1, \dots, N_1\}, j \in \{1, \dots, N_2\}$ **do**
        $\overline{w}^{ij}_{I,t} \leftarrow \dfrac{\widetilde{w}^{ij}_{I,t} \cdot w^{ij}_{I,t-1}}{\sum_{i=1}^{N_1} \sum_{j=1}^{N_2} \widetilde{w}^{ij}_{I,t} \cdot w^{ij}_{I,t-1}}$
    foreach $i \in \{1, \dots, N_1\}$ **do**
        $\delta \leftarrow \text{rand}((0; N_2^{-1}))$
        $cdf \leftarrow 0$, $k \leftarrow 0$, $c_j \leftarrow []$ for all j
        for $j = 0$, $j < N_2$ **do**
            $u \leftarrow \delta + j \cdot N_2^{-1}$
            while $u > cdf$ **do**
                $k \leftarrow k + 1$
                $cdf \leftarrow cdf + \overline{w}^{ik}_{I,t}$
            $c_{j+1} \leftarrow k$
        for $j = 1$; $j \leq N_2$ **do**
            $w^{ij}_{I,t} \leftarrow \frac{c_j}{N_2}$
    return $\{\{w^i_{B,t} \cdot w^{ij}_{I,t}\}_{j=1}^{N_2}\}_{i=1}^{N_1}$

VII. NUMERICAL SIMULATIONS

In this section, we present a suite of multi-agent deployment-map updating simulations with different sensor models.

Gaussian PDFs for the Observation Likelihood: For the simulation, we consider Gaussian kernels for the probability distributions of both the perception model, and the detection model. First, consider the conditional probability distribution for detection likelihood, positive and negative functions respectively

$$p_{\boldsymbol{y}^i_{B,t}|x_t, \boldsymbol{q}}(\boldsymbol{y}^i_{B,t} = 1 \mid x_t, \boldsymbol{q} = q) = \eta_B \mathcal{N}(q, x^i_t, \Sigma_B)$$
$$= \eta_B \frac{1}{2\pi |\Sigma_B|} \exp\left(\frac{-(q - x^i_t)^\top \Sigma_B^{-1}(q - x^i_t)}{2} \right),$$
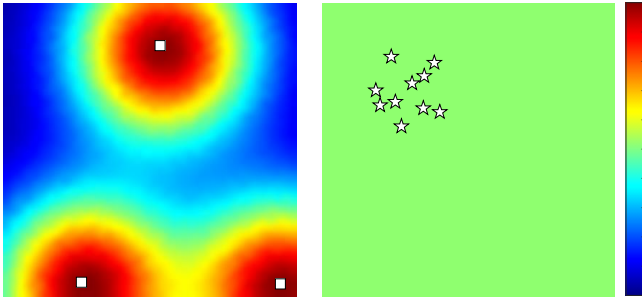
Fig. 1: Left: the expected target intensity (the ground truth), right: initial configuration of 10 robots where background color (gray) shows spatial density for every target is uniform. Squares in the left are the peaks of the mixture of Gaussians, and stars on the right are the robots' locations
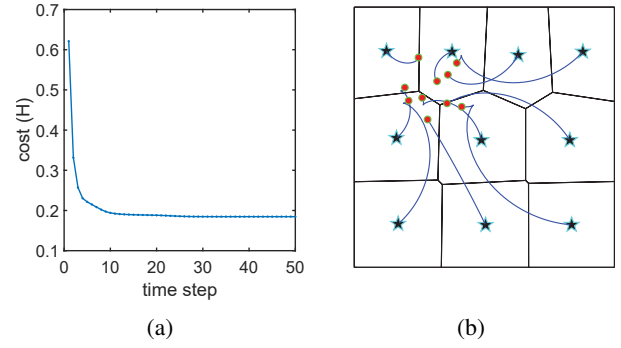

(a)   (b)

Fig. 2: One-time deployment, (a) cost change during Algorithm 1, (b) optimal path respecting unicycle kinematic constraint (small circles: initial positions, stars: target positions, solid lines: partitions at target positions)

and

$$p_{\boldsymbol{y}_{B,t}^i | x_t, \boldsymbol{q}}(\boldsymbol{y}_{B,t}^i = 0 \mid x_t, \boldsymbol{q} = q) = 1 - \eta_B \mathcal{N}(q, x_t^i, \Sigma_B)$$

where $\mathcal{N}(q, x_t^i, \Sigma_B)$ is multivariate Gaussian with mean x_t^i and covariance matrix Σ_B, and η_B is a constant. Assume that the noisy sensor model is also a multi-variate Gaussian with mean $y_{I,t}^i$ and covariance matrix Σ_I.

$$f_{\boldsymbol{y}_{I,t}^i | x_t, \boldsymbol{I}}(y_{I,t}^i \mid x_t, \boldsymbol{I} = I) = \eta_I \mathcal{N}(I, y_{I,t}^i, \Sigma_I)$$

where η_I is normalization constant. The total observation likelihood is given by

$$
\begin{aligned}
&f_{\boldsymbol{y}_t^i | x_t, \boldsymbol{z}}\left(y_{B,t}^i, y_{I,t}^i \mid x_t, \boldsymbol{z} = (q, I)\right) \\
&= \begin{cases}
\eta_B \eta_I (1 - \mathcal{N}(q, x_t^i, \Sigma_B)) \mathcal{N}(I, y_{I,t}^i, \Sigma_I), & \text{if } y_{B,t}^i = 0 \\
\eta_B \eta_I \mathcal{N}(q, x_t^i, \Sigma_B) \mathcal{N}(I, y_{I,t}^i, \Sigma_I), & \text{if } y_{B,t}^i = 1
\end{cases}
\end{aligned}
$$

Simulation settings: In the simulation, we consider $\mathcal{Q}$ be a unit square space $[0, 1] \times [0, 1]$ in $\mathbb{R}^2$, $\mathcal{I} = [0, 1]$, and $r_{\text{eff}} = 0.2$ (or ∞ if it is relaxed). Targets are uniformly distributed over $\mathcal{Q}$, and the initial expected spatial density of the target over $\mathcal{Q}$ is given in Fig. 1 (left) as a mixture of Gaussian kernels. The intensity of the expected spatial distribution ranges from 0 to 1, which corresponds to black to white colored areas, respectively. The empty square denotes the peak of each kernel. As shown in Fig. 1 (right), at time 0, 10 mobile robots are deployed at the upper-left corner of $\mathcal{Q}$ where the empty star denotes the robots' positions. We assume that there is no prior knowledge of the target information such that color intensity is also uniformly set to 0.5 out of 1. A number of particles used for the SIR filter is $N = N_1 \times N_2 = 1000 \times 100$. The value of the equipped noisy sensor's covariance matrix is fixed at $\Sigma_I = 0.5\mathbf{I}$, and the binary sensor's covariance is fixed at $\Sigma_B = 0.04\mathbf{I}$ where $\mathbf{I} \in \mathbb{R}^{d \times d}$ is an identity matrix.

Convergence of deployment algorithm: First, the behavior of the deployment strategy is discussed. Given the initial uniform prior belief, robots is governed by the gradient descent strategy (Algorithm 1) to obtain the next way-point x_1 for the next time step 1. As previously noted in the Section V, robots move toward the locations which maximize the likelihood of positive detections. Fig. 2(a) shows the convergence of the algorithm,

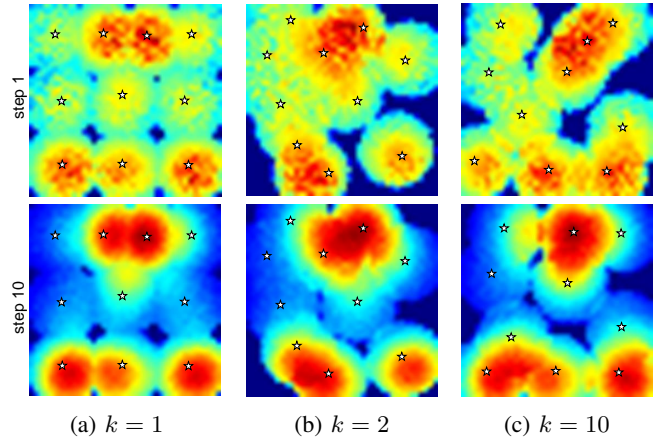(a) $k = 1$ (b) $k = 2$ (c) $k = 10$

Fig. 3: Belief propagation using various methods with moderate detection range where $r_{\text{eff}} = 0.2$, $\Sigma_B = 0.04\mathbf{I}$ ((a) $k = 1$, (b) $k = 2$, (c) $k = 10$, the 1st row: step 1, the 2nd row: step 10, stars: positions of robots at 10th step)

and Fig. 2(b) illustrates the path generated by optimal control low when each robot has unicycle kinematics.

Filtering performance: Next, we present the evolution of the object map given the uniform, initial map (Fig. 1(right)) with successive positive observations, each followed by the gradient descent strategy and filtering process. Fig. 3 illustrates the map building process, given limited effective sensing range value ($r_{\text{eff}} = 0.2$, the value was chosen empirically relative to the workspace size) by different methods with $k = 1, 2, 10$ respectively, by showing robots' positions and the current belief at time step 1 and 10 respectively. The results depicted in Fig. 3 clearly show that under *limited sensing range*, the non-coordinated strategy ($k = 1$) yields relatively better mapping results than coordinated strategies ($k = 2, 10$) compared to the ground truth map shown in Fig 1(left). In addition, Fig. 4(a) compares the K-L divergence values between different strategies during the evolution when $r_{\text{eff}} = 0.2$. We included the results with 2D random walk with step size 0.2 to illustrate the performance gain from our algorithm. Finally, Fig. 4(b) compares the K-L divergence values between different strategies when $r_{\text{eff}} = \infty$ merely to illustrate the filtering performance when the constraint
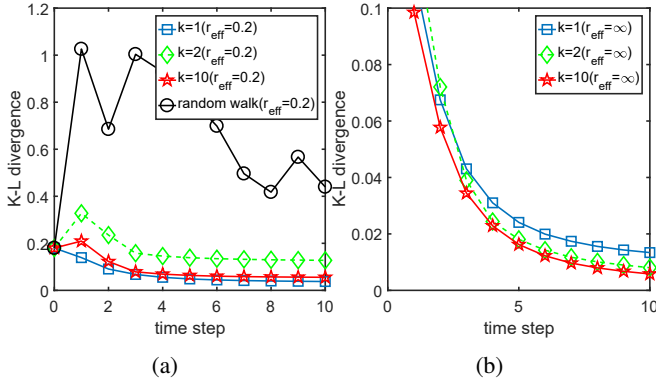
Fig. 4: Comparison of K-L divergence from the actual distribution between different sensor models during belief propagation; (a) $r_{\text{eff}} = 0.2$, (b) $r_{\text{eff}} = \infty$
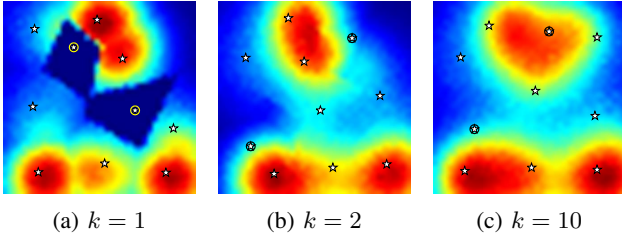

(a) $k = 1$ (b) $k = 2$ (c) $k = 10$

Fig. 5: Comparison of robots' configuration and beliefs at the final step with two approaches, $k = 1, 2, 10$ when two of the sensors fails (circled) and $r_{\text{eff}} = \infty$, $\Sigma_B = 0.04\mathbf{I}$ for both cases

on the sensing range is relaxed. As can be seen, in this case, coordinate strategies yields better performance than the the non-coordinate one. We also note that in all cases, our deployment strategies has noticeably improved the quality of the map along the evolutions. The occurrence of sudden jumps (between the time step 0 and 1) in the K-L divergence values observed in Fig 4(a) demonstrates the cases when the initial uniform density happened to a better '*guess*' than the crude belief obtained after a single propagation of the filtering process.

Robustness to sensor failure: As seen in the previous section, despite the relatively higher sensing cost seen from the coordinated methods than the non-coordinated method
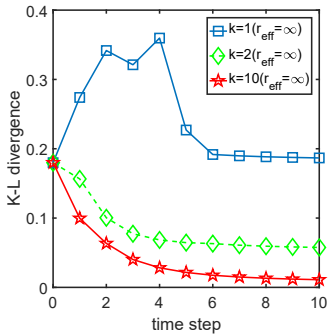

Fig. 6: Comparison of K-L divergence from the ground-truth distribution between multiple strategies ($k = 1, 2, 10$), when two sensors fail, during the evolution

($k = 1$), performances are even worse for the range-limited case. This section presents an example when the coordinated strategy becomes more desirable. And, this happens when the sensors are not perfect and likely to fail to detect a target. Results for configurations and spatial distributions after 10th step with $k = 1, 2, 10$, are shown in Fig. 5(a)-(c), respectively. To reveal the full potential of the coordinated strategies, we relaxed the effective sensing range constraint, such that $r_{\text{eff}} = \infty$. As can be seen from Fig 5 and Fig. 6, the map retrieved by the coordinated strategies $k = 2, 10$ are more accurate, and more robust to the sensor failure compared to that obtained with the non-coordinated strategy. Due to its fully decentralized nature, it is not surprising to see from this example that the non-coordinated method ($k = 1$) works poorly under the sensor failures.

VIII. CONCLUSIONS AND FUTURE WORK

In this paper, we have presented a general deployment strategy for a fleet of autonomous vehicles for maximum recovery of spatial distribution map over a bounded space. It is expected that our method will fail if there are not enough number of mobile agents having long enough effective sensing ranges relative to the workspace size. One of our future works is, therefore, to develop multi-agent patrolling algorithms (see e.g., [22]) to compensate such problems where there are not enough number of sensors to cover the whole target space. Also, as reported in the literature [12], our combined sensor model can be used to model the real-world laser scanner's behavior, nevertheless, it is one of our future works to conduct extensive real world multi-robot experiments for further validation of our range sensor model. Lastly, we assumed in this study that the beliefs are shared between robots such that both tasks of propagating and approximating belief require a central entity. It is one of our future works to devise distributed communication protocol to enable distributed belief estimation.

¡¡¡¡¡¡¡ Updated upstream ======= ¿¿¿¿¿¿¿ Stashed changes

REFERENCES

[1] S. S. Dhillon and K. Chakrabarty, "Sensor placement for effective coverage and surveillance in distributed sensor networks," in *Wireless Communications and Networking, 2003. WCNC 2003. 2003 IEEE*, vol. 3. IEEE, 2003, pp. 1609–1614.

[2] A. Howard, M. J. Matarić, and G. S. Sukhatme, "Mobile sensor network deployment using potential fields: A distributed, scalable solution to the area coverage problem," in *Distributed autonomous robotic systems 5*. Springer, 2002, pp. 299–308.

[3] J. Cortés, S. Martínez, T. Karatas, and F. Bullo, "Coverage control for mobile sensing networks," *Robotics and Automation, IEEE Transactions on*, vol. 20, no. 2, p. 243255, 2004.

[4] L. Yu, N. Wang, and X. Meng, "Real-time forest fire detection with wireless sensor networks," in *Wireless Communications, Networking and Mobile Computing, 2005. Proceedings. 2005 International Conference on*, vol. 2. IEEE, 2005, pp. 1214–1217.

[5] F. Bourgault, T. Furukawa, and H. F. Durrant-Whyte, "Coordinated decentralized search for a lost target in a bayesian world," in *Intelligent Robots and Systems, 2003.(IROS 2003). Proceedings. 2003 IEEE/RSJ International Conference on*, vol. 1. IEEE, 2003, pp. 48–53.

[6] L. D. Stone, R. L. Streit, T. L. Corwin, and K. L. Bell, *Bayesian multiple target tracking*. Artech House, 2013.

[7] S. Candido, J. Davidson, and S. Hutchinson, "Exploiting domain knowledge in planning for uncertain robot systems modeled as pomdps," in *Robotics and Automation (ICRA), 2010 IEEE International Conference on*. IEEE, 2010, pp. 3596–3603.

[8] B. Ristic, M. Morelande, and A. Gunatilaka, "Information driven search for point sources of gamma radiation," *Signal Processing*, vol. 90, no. 4, pp. 1225–1239, 2010.

[9] J.-M. Valin, F. Michaud, and J. Rouat, "Robust localization and tracking of simultaneous moving sound sources using beamforming and particle filtering," *Robotics and Autonomous Systems*, vol. 55, no. 3, pp. 216–228, 2007.

[10] A. J. Lilienthal, M. Reggente, M. Trincavelli, J. L. Blanco, and J. Gonzalez, "A statistical approach to gas distribution modelling with mobile robots-the kernel dm+ v algorithm," in *Intelligent Robots and Systems, 2009. IROS 2009. IEEE/RSJ International Conference on*. IEEE, 2009, pp. 570–576.

[11] P. M. Djuric, M. Vemula, and M. F. Bugallo, "Target tracking by particle filtering in binary sensor networks," *IEEE Transactions on Signal Processing*, vol. 56, no. 6, pp. 2229–2238, 2008.

[12] D. Anguelov, D. Koller, E. Parker, and S. Thrun, "Detecting and modeling doors with mobile robots," in *Robotics and Automation, 2004. Proceedings. ICRA'04. 2004 IEEE International Conference on*, vol. 4. IEEE, 2004, pp. 3777–3784.

[13] S. Hutchinson and T. Bretl, "Robust optimal deployment of mobile sensor networks," in *Robotics and Automation (ICRA), 2012 IEEE International Conference on*, 2012, p. 671676.

[14] M. Schwager, D. Rus, and J.-J. Slotine, "Decentralized, adaptive coverage control for networked robots," *The International Journal of Robotics Research*, vol. 28, no. 3, pp. 357–375, 2009.

[15] H. Park and S. Hutchinson, "Robust optimal deployment in mobile sensor networks with peer-to-peer communication," in *Robotics and Automation (ICRA), 2014 IEEE International Conference on*. IEEE, 2014, pp. 2144–2149.

[16] M. I. Shamos and D. Hoey, "Closest-point problems," in *Foundations of Computer Science, 1975., 16th Annual Symposium on*. IEEE, 1975, pp. 151–162.

[17] J. Beardwood, J. H. Halton, and J. M. Hammersley, "The shortest path through many points," in *Mathematical Proceedings of the Cambridge Philosophical Society*, vol. 55, no. 04. Cambridge Univ Press, 1959, pp. 299–327.

[18] S. M. LaValle, *Planning algorithms*. Cambridge university press, 2006.

[19] M. S. Arulampalam, S. Maskell, N. Gordon, and T. Clapp, "A tutorial on particle filters for online nonlinear/non-gaussian bayesian tracking," *IEEE Transactions on signal processing*, vol. 50, no. 2, pp. 174–188, 2002.

[20] D. Crisan and A. Doucet, "A survey of convergence results on particle filtering methods for practitioners," *IEEE Transactions on signal processing*, vol. 50, no. 3, pp. 736–746, 2002.

[21] H. M. Choset, *Principles of robot motion: theory, algorithms, and implementation*. MIT press, 2005.

[22] D. Portugal and R. Rocha, "A survey on multi-robot patrolling algorithms," in *Doctoral Conference on Computing, Electrical and Industrial Systems*. Springer, 2011, pp. 139–146.